LOW TEMPERATURE SOLDERING: REFLOW OPTIMIZATION FOR ENHANCED MECHANICAL RELIABILITY

Morgana Ribas, Ph.D., Bhaskar Vangapandu, Raghu Raj Rangaraju, Suresh Telu, Ph.D., Laxminarayana Pai, Ramesh Kumar, Vikas Patil, H. V. Ramakrishna, Ph.D., Traian Cucu, Ph.D., Siuli Sarkar, Ph.D.
Alpha Assembly Solutions, a MacDermid Performance Solutions Business
Bangalore, India
siuli.sarkar@alphaassembly.com

ABSTRACT
There is a growing interest surrounding use of Sn-Bi solder alloys for lowering reflow soldering temperature. Among the many benefits enabled by that are: Reduced dynamic warpage, more complex assemblies, reduced energy costs and increased production yields. Recently, low temperature solder alloys with micro-additives have been introduced as an alternative for replacing Sn-Ag-Cu solders while maintaining its mechanical (drop) shock performance. In this work, we further discuss solderability and mechanical reliability of a novel low temperature proprietary alloy (generically called as X46). Its drop shock performance evaluation is extended to include the effect of various reflow profiles, including the effect of time above liquidus (TAL) and peak reflow temperatures. Analysis of soldering performance, including voids measurements, and failure analysis are also included in the discussion. Based on these results, the following reflow conditions are recommended: (i) For BGA, peak temperature of 190-200^{o}C (±3^{o}C) and TAL between 30 and 90s, (ii) For the LGA, 180-200^{o}C (±3^{o}C) peak temperature and TAL between 30 and 90s.

Key words: Lead-free, low temperature soldering, Sn-Bi alloys, drop shock, voids, reflow optimization.

INTRODUCTION
A growing interest on using low temperature alloys to replace Sn-Ag-Cu solders has motivated extensive research on development of new low temperature solder pastes [1-4]. Such new solder alloys and pastes can be used for lowering reflow soldering temperature and, consequently, reducing dynamic warpage, energy costs and increasing production yields [5-9]. Indeed, the 2017 iNEMI roadmap predicts that low-temperature solder pastes usage will grow from less than about 1% to 10% by 2021, potentially reaching 20% by 2027 [10]. The eutectic 42Sn58Bi alloy has melting point around 138^{o}C and can be reflowed between 175-185^{o}C, and was considered as a SnPb replacement at the transition to Pb-free. However, it was not an ideal Pb-free alternative given its drawbacks, including brittleness, and drop shock and fatigue life lower than SAC305 [11-13].

In this work, we further discuss solderability and mechanical reliability of a novel low temperature proprietary alloy (generically called as X46). The melting behaviour and microstructure of a SnBi alloy affects its ability to form a mixed solder joint with Sn-Ag-Cu alloys. DSC analysis showed that Bi content should be equal or higher than 40 wt.% for enabling reflow profiles with peak temperature lower than 200^{o}C [14-15]. Cross-section analysis of SAC305 spheres assembled with X46 solder paste showed that solder joints reflowed using 190^{o}C peak temperature achieved better inter-diffusion, i.e., mixing [14]. Real-time imaging of mixed solder joints reflow was performed to better understand the formation of mixed solder joints [16]. Figure 1(a) shows real-time imaging snap shots taken during reflow of X46 solder paste and SAC305 spheres. It confirms DSC results, showing X46 solder paste starts melting at 139^{o}C (+/-1^{o}C) and is completely liquid at 150^{o}C (+/-1^{o}C). In addition to that, it shows partial collapse of the SAC305 sphere at 188^{o}C (+/-1^{o}C), indicating an increased inter-diffusion with X46 alloy. This is further confirmed by real-time imaging taken when reflowing X46 solder paste and eutectic Sn-Bi spheres, shown in Figure 1(b), in which X46 is almost completely in the liquid state at 142^{o}C.

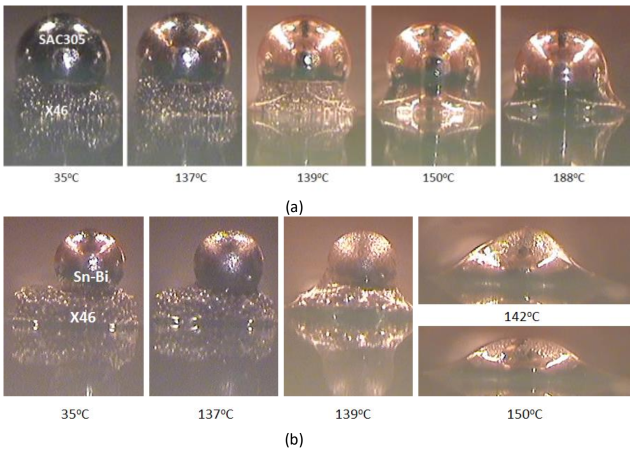

Figure 1. Real-time images of (a) mixed X46/SAC305 solder joint during reflow and (b) SnBi/X46 solder joint during reflow [16].

Based on this information, 190°C peak reflow appears as the logical choice for reflowing mixed X46/SAC305 solder joints. However, inter-diffusion will also happen (in a lower degree) when reflowing assemblies at 180°C, whereas the complete mixing between SAC305 and X46 will occur when reflowing at 200°C [14]. Thus, soldering low temperature and Sn-Ag-Cu solder alloys is possible within 180 and 200°C peak temperatures, but how good are these solder joints? To answer this and other questions, this work evaluates the effect of nine reflow profiles, in which the effect of time above liquidus (TAL) and peak reflow temperatures on basic solder joint properties and mechanical drop shock reliability are evaluated.

EXPERIMENTAL DESCRIPTION

Bulk Alloy Testing

Solidus and liquidus temperatures are measured using a Differential Scanning Calorimeter (DSC), as per ASTM E794 standard [17]. Multiple samples of each alloy are evaluated and the melting range is given as the interval between the solidus and liquidus temperatures.

Tensile tests were conducted using a universal testing machine, using rounded specimens prepared as per ASTM E8 [18] tensile test standard (16 mm gauge length and 4 mm diameter), as shown in Figure 2. Average values of ultimate tensile strength, yield strength and elongation are obtained from stress-strain curves of at least five specimens. The test is conducted at room temperature using 10^{-3} s^{-1} strain rate. The Young's modulus is calculated based on the density of the material and the sound velocity measured through the alloy. For that, an ultrasonic thickness gauge, and longitudinal and shear wave transducers are used.

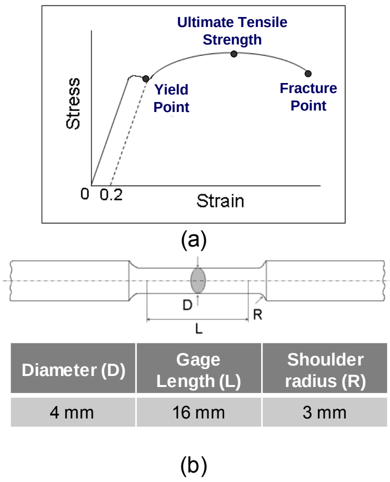

Figure 2. (a) Schematic stress-strain curve and (b) details of specimens used in the tensile test.

The creep test was conducted at 85°C, under 150N load. Prior to the testing, cylindrical specimens of 9 mm gauge length and 6 mm diameter were machined and baked at 85°C for 48 hrs. Creep curves of strain versus time are recorded and the maximum time before rupture (i.e., creep strength) and maximum elongation (i.e., creep elongation) are reported as the average values of at least three specimens.

Solder Joint Evaluation

Test vehicles used for evaluating solderability and drop shock performance were assembled using nine different reflow profiles, as described in Table 1. Three reflow peak temperatures are used, 180±3°C, 190±3°C and 200±3°C (Figure 3), in which the reflow temperature is raised about 30 to 50°C above the liquidus temperature. The time above liquidus (TAL) is kept at 30-45s, 90s and 120s.

Table 1. Details of the nine reflow profiles used.

Profile ID.	Peak Temp., °C	TAL, sec
A	180	30-45
B	180	90
C	180	120
D	190	30-45
E	190	90
F	190	120
G	200	30-45
H	200	90
I	200	120

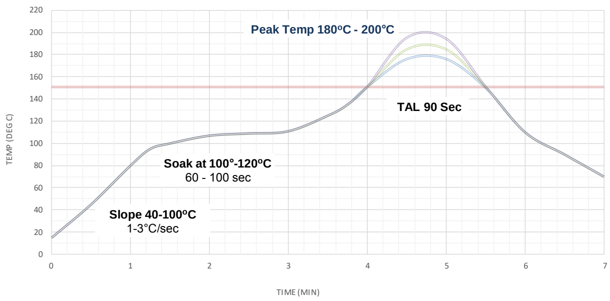

Figure 3. Reflow profiles showing the three peak temperatures used in this study.

Voids are measured using X-ray and classified as per IPC-7095A standard [19]. The random solder ball (RSB) test evaluates how a solder paste reflow and coalesce on a non-wettable substrate. After printing the solder paste on a ceramic testing coupon, samples are reflowed immediately after printing or after 4 hrs (±15 min) conditioning at 25°C ±3°C and 50%± 10% RH. After reflowing, the visual appearance of the samples is compared to the classification defined in the IPC TM-650 2.4.43 standard [20].

The cross-print test evaluates the wetting of a solder paste. Pairs of solder paste stripes are printed perpendicularly to a pattern of copper pads and solder mask stripes. Each pair of stripes is spaced between 0.3 mm and 1.0 mm (in 0.1 mm increments). Upon reflow the solder paste printed on the mask pulls back to the pad and may touch each other, depending on the spacing between the traces. The cross-print wetting performance is given by counting the number of shorts (up to 20) for each space interval.

The solder joint cosmetics is obtained by visually inspecting the solder and paste flux residue when using the various reflow profiles. They are inspected for gathering information on flux residue colour, flux residue characteristics, presence or not of random solder ball on the mask, solder cosmetics and wetting on large pad.

Solder Joint Reliability

The JEDEC standard JESD22-B111 was used for testing the effect of drop on solder joints at board level [21]. Each Cu-OSP finished test vehicle is assembled with a total of seven CTBGA84 components. The BGAs use 12 mil SAC305 solder spheres in an array with 0.5 mm pitch. The drop shock testing machine is set by adjusting the drop height and striking surface to JEDEC's recommended condition (1500 Gs, 0.5 msec duration and half-sine pulse). The electrical continuity of each component is monitored by using a high-speed event detector. Each component is tested till its complete failure, as defined in the I PC/JEDEC-9706 standard for Mechanical Shock In-situ
Electrical Metrology Test [22].

RESULTS AND DISCUSSION

Bulk Alloy Testing

Table 2 shows some key physical properties of alloy X46, including melting behaviour, tensile strength and high temperature creep. The melting point of the eutectic 42Sn58Bi alloy is about 138°C. Other Sn-Bi alloys with lower Bi content generally have higher liquidus temperature, depending on micro-alloying additions. In the case of alloy X46, which is a non-eutectic Sn-Bi solder with 2 wt.% additives, the solidus and liquidus temperatures are 138°C and 151°C, respectively. Additionally, a DSC curve of X46 shows a 79.7% conversion into liquid at 139°C and 99% at 144°C [14].

Table 2. Physical properties of X46 solder alloy.

Alloy	X46	SAC305
Melting Temperatures (°C)	138-151	217-220
Ultimate Tensile Strength (MPa)	62.2	44.5
Yield Strength (MPa)	37.5	39.6
Elongation (%)	40.8	46.1
Young's Modulus (GPa)	41.4	49.8
Creep Strength (hrs)	26.0	-

Standard deviations for the average values of ultimate tensile strength, yield strength and elongation are lower than 2.2 MPa, 4.5 MPa and 7.6%, respectively. X46 alloy ultimate tensile strength is higher than SAC305, but similar to other Sn-Bi alloys [23]. Its elastic modulus is slightly higher than other Sn-Bi alloys evaluated in previous studies, but much lower than SAC305. However, unlike other Sn-Bi alloys its yield strength and elongation at room temperature are within standard deviation of the values obtained for SAC305.

Creep curves obtained from the high temperature creep test show a very short stage I (dominated by strain hardening), with a longer stage II (almost constant deformation), followed by a quick stage III (necking and rupture). The creep strength is given by the average creep rupture time. X46 creep strength is almost twice of the 42Sn-57.6Bi-0.4Ag alloy [23], which serves as an indicator of its better fatigue life and better thermal cycling performance.

Solder Joint Evaluation

Using the reflow profiles A to I described in Table 1, voids analysis of BGA256 and MLF100, IPC RSB, cross-print wetting and the overall appearance of the solder joint were evaluated. Although it is common for BGA voids to be classified as IPC class 3, the reflow profiles with extended TAL of 120s resulted in higher voids for all three peak temperatures, as showed in Figure 4(a), some of which are classified as IPC class 2. The voids in BGA reflowed with the remaining profiles are classified as IPC class 3. There are very little differences among profiles A, B, D and E using 30-45s and 90s TAL at 180°C and 190°C peak. Profiles G and H are also classified as class 3, but have somehow more voids, highlighting the effect of peak temperature. Unlike in the BGA where 256 data points are available in each component, only the overall degree of voids for two components is reported for the MLF components in Figure 4(b). The % voids in the MLF 100 is very similar, showing less effect of the reflow profile than in the BGA256. However, the respective images of these solder joints show an increase in the number of voids (smaller in size) for the higher TAL of 120s. It is interesting to note that solder joints in the BGA256 are mixed X46/SAC305, whereas in the MLF 100 they are only homogeneous X46 alloy.

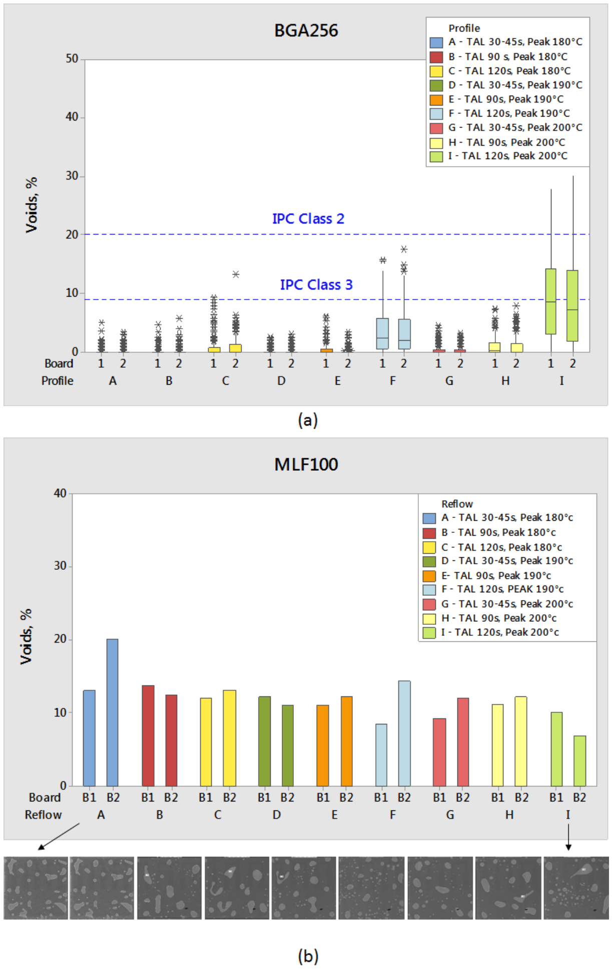

Figure 4. Voids (a) BGA256 and (b) MLF100.

The IPC RSB results when the coupons are reflowed immediately after printing or after conditioning are showed in Figure 5. Except for the reflow profiles having 120s TAL (i.e., C, F and I) after conditioning, all other profiles pass the IPC criteria of preferred and acceptable RSB, having soft and clear flux residues. The profiles with 120s TAL do not meet IPC criteria, having unacceptable RSB and clusters and soft and light amber colour residues.

Figure 6 shows the cross-print wetting for the various reflow profiles. In general, an ideal cross-print wetting is above 75-80% at 0.6 mm spacing between two traces, i.e., 75-80% of the traces spaced at 0.6 mm would bridge. All the nine profiles fulfil this ideal performance. The peak reflow temperature has little or no effect on the cross-print wetting. For example, a TAL 30-45s results in 80, 80 and 83% bridges for 180, 190 and 200°C, respectively. However, the cross-print wetting is considerable higher for much higher TAL of 120s, 93% for 180 and 190°C and 98% for 200°C.

An example of the respective solder joints appearance on the cross-print pattern is showed in Figure 7. No random solder balls are observed in the mask for profiles with 30-45s and 90s TAL in all three peak temperatures (A, B, D, E, G and H. However, solder balls were observed for the profiles using 120s TAL (C, F and I). Another example of solder joint appearance and good wetting is showed in Figure 8, for the QFP208. All pads have good solder coverage and no exposed pads were observed. Overall, the flux residue has the same appearance using all the nine profiles, soft and colourless.

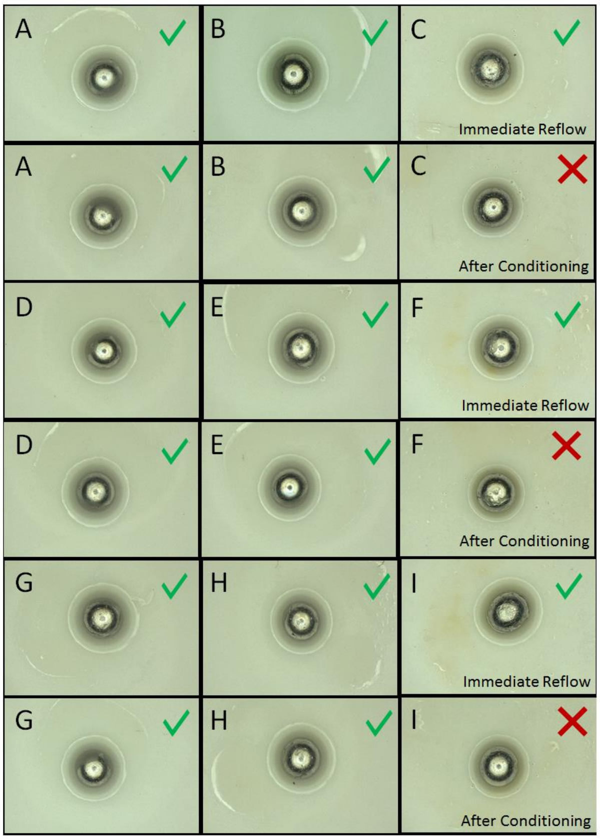

Figure 5. Images from IPC random solder ball evaluation.

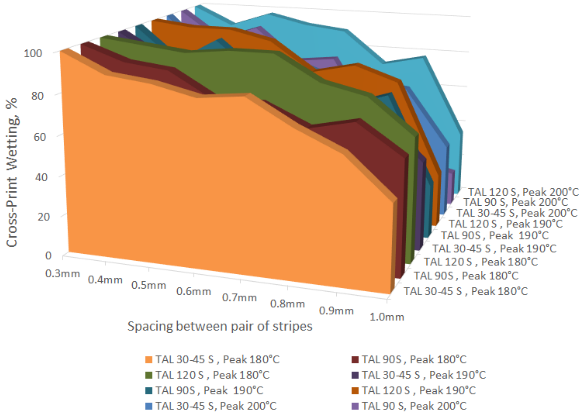

Figure 6. Cross-print wetting for the various reflow profiles.

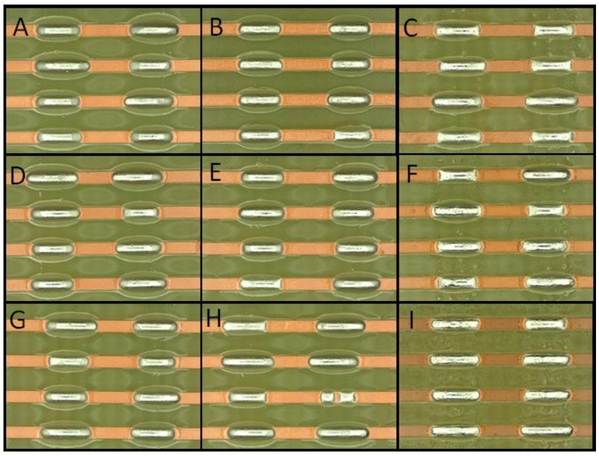

Figure 7. Solder joint appearance on the cross-print pattern.

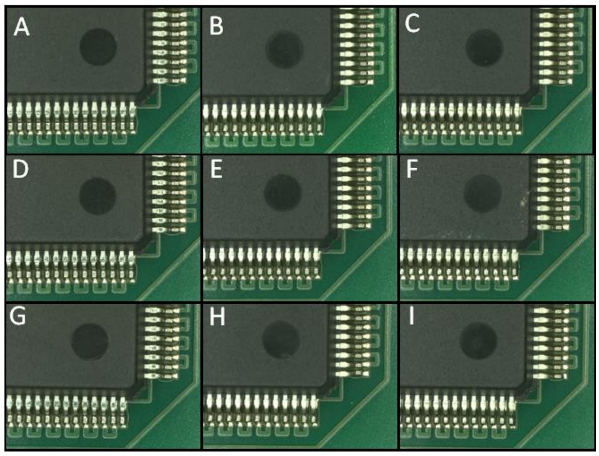

Figure 8. Solder joint appearance for QFP208.

Effect of Reflow Profile on Drop Shock

Figure 9 to 11 show the effect on the drop shock performance of 180, 190 and 200°C peak reflow temperatures, respectively, for the three TAL conditions. The drop shock characteristic life (63.2% failures) of BGA84 and LGA84 for each profile is obtained from the Weibull plot and the data is analysed considering a 90% confidence interval in each distribution.

The drop shock characteristic life varies significantly for BGA and LGA at 180°C (Figure 9). Reflowing BGA84 with profiles with 30-45s and 90s TAL resulted in considerably lower drop shock (337 and 264 drops, respectively) than 120s TAL for BGA (556 drops) and any of the LGA (727 to 935 drops). Using 90s and 120s TAL at 180°C for the LGA84 also results in higher drop shock than for the BGA84 using 120s TAL (556 drops). For 190°C peak temperature, the drop shock characteristic life is between 684 and 926 drops, for both BGA and LGA (Figure 10). The 190°C peak temperature was found to be more flexible, as choosing a TAL of 30-45s, 90s or 120s resulted in drop shock characteristic lives within overlapping confidence intervals. At 200°C (Figure 11), the only significant difference in drop shock characteristic life was observed between 120s TAL for BGA84 (571 drops) and 30s TAL for LGA84 (871 drops).

A summary of the failure analysis of these components after drop shock testing is showed in Figure 12 and 13, for BGA84 and LGA84, respectively. At 190°C peak, the failure is localized at the interface between the copper pad and the Sn-Bi solder paste, mostly through the Cu_6Sn_5 intermetallics. However, when the TAL is increased to 120s, the failure shifts to the package side, perhaps due to an increase in the mixing between the SAC305 sphere and the Sn-Bi solder paste. Mixed failure modes are observed in BGA at 180 and 200°C peak. The reasons for that are still under investigation, but poor Sn-Bi/SAC mixing (in the case of 180°C peak) or excessive Sn-Bi/SAC mixing (for 200°C) are some of the possibilities. In the case of the LGA84, apparently there is no preferred path for the cracks to initiate and propagate, which can be either on bulk, package or PCB side, as exemplified in Figure 13.

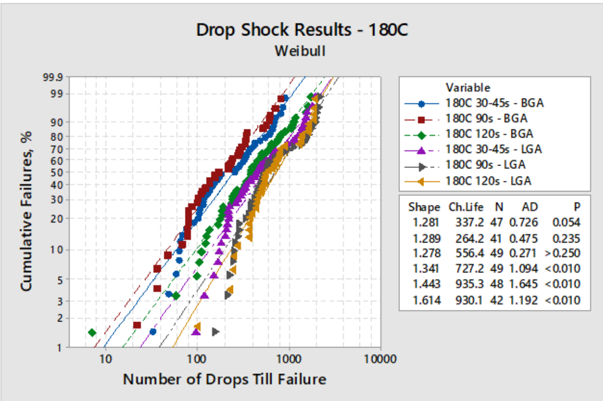

Figure 9. Drop shock results using reflow peak at 180°C.

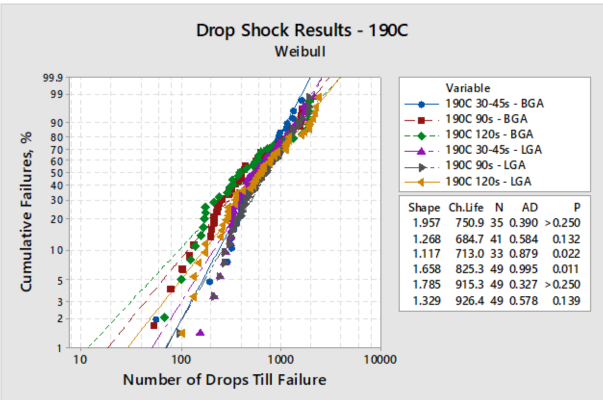

Figure 10. Drop shock results using reflow peak at 190°C.

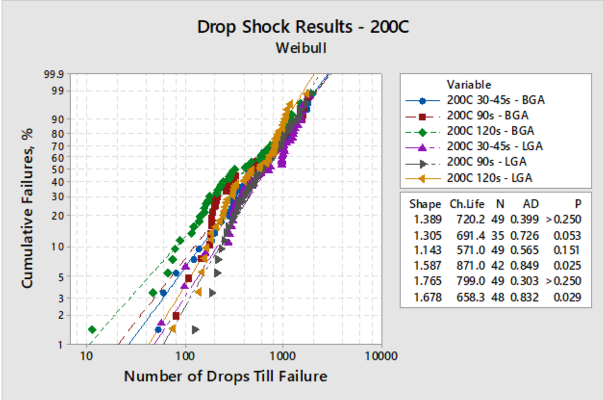

Figure 11. Drop shock results using reflow peak at 200°C.

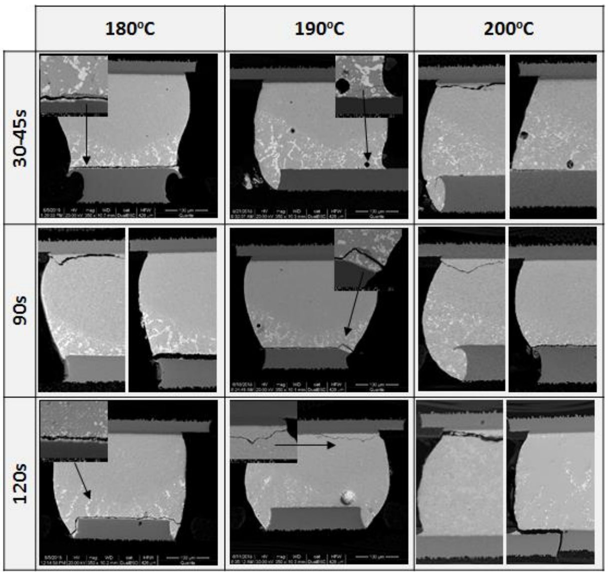

Figure 12. Failure analysis of BGA84 after drop shock.

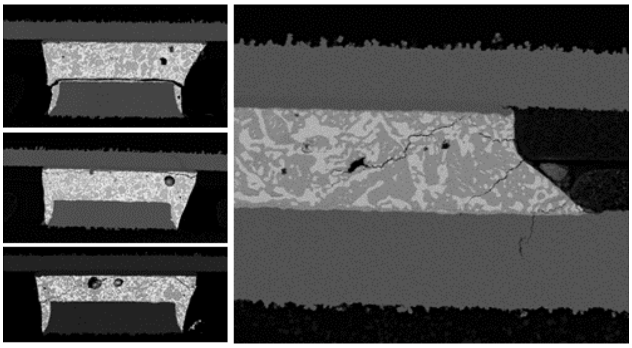

Figure 13. Failure analysis of LGA84 after drop shock.

From these drop shock results, we can also conclude that it is not possible to achieve the maximum BGA84 drop shock performance using a peak reflow temperature of 180°C and 30-45s or 90s TAL. However, for the LGA84, except for the profile with 200°C peak and 120s TAL, all profiles achieved its maximum drop shock characteristic life (727 to 935 drops). Considering these and solderability results, the recommended reflow conditions for BGA assembly have peak temperature of 190-200°C and TAL between 30 and 90s (Figure 14). For the LGA, 180-200°C peak temperature and TAL between 30 and 90s are recommended.

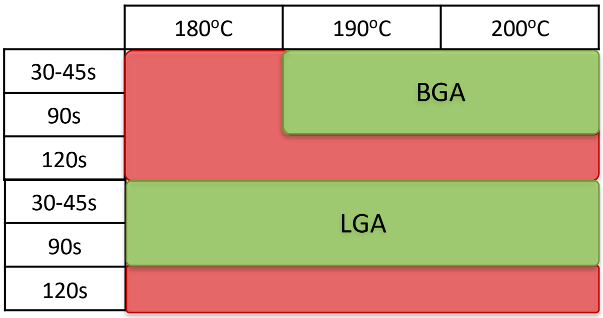

Figure 14. Recommended reflow profiles for BGA and LGA. (Green: recommended, Red: not recommended)

CONCLUSIONS

In this work, we investigated the effect of various reflow profiles on solderability and solder joint mechanical shock reliability. Its key observations are:

- Extended TAL of 120s results in more voids in BGA256 and does not pass IPC RSB test after 4 hrs conditioning.
- LGA84 can be reflowed at 180, 190 or 200°C peak temperature using 30 to 120s TAL, without degradation of mechanical shock performance.
- Mixed failure mode was observed for BGA reflowed at 180 and 200°C, but all BGA reflowed at 190°C showed cracks through the IMC after the drop shock test.
- BGA84 can be reflowed at 190 or 200°C peak temperature using 30 to 120s TAL (or 30 to 90s TAL in case of 200°C peak), without degradation of mechanical shock performance.

Therefore, the recommended reflow conditions are (i) For BGA assembly, peak temperature of 190-200°C (±3°C) and TAL between 30 and 90s, (ii) For the LGA, 180-200°C (±3°C) peak temperature and TAL between 30 and 90s.

ACKNOWLEDGEMENTS

We thank our colleagues at the India R&D Centre for their key support to this work. We are also grateful to other colleagues that eventually have participated in the discussion of the work from which this manuscript is derived.

REFERENCES

[1] H. Fu, R. Aspandiar, J. Chen, S. Cheng, Q. Chen, R. Coyle, S. Feng, M. Krmpotich, R. Lasky, S. Mokler, J. Radhakrishnan, M. Ribas, B. Sandy-Smith, K. K. Tang, G. Wu, A. Zhang, and W. Zhen, "iNEMI Project on Process Development of BiSn-Based Low Temperature Solder Pastes", Proceedings of the 2017 SMTA International Conference, Rosemont, IL, September 2017, 207-220.

[2] H. Fu, R. Aspandiar, J. Chen, S. Cheng, Q. Chen, R. Coyle, S. Feng, B. Hardin, M. Krmpotich, S. Mokler, J. Radhakrishnan, M. Ribas, B. Sandy-Smith, K. K. Tang, G. Wu, A. Zhang, and W. Zhen, "iNEMI Project on Process Development of BiSn-Based Low Temperature Solder Pastes – Part II: Characterization of Mixed Alloy BGA Solder Joints", Proceedings of the 2018 Pan Pacific Microelectronics Symposium, Hawaii, February 2018.

[3] H. Fu, J. Radhakrishnan, M. Ribas, R. Aspandiar, K. Byrd, J. Chen, S. Cheng, Q. Chen, R. Coyle, S. Feng, B. Hardin, M. Krmpotich, S. Mokler, B. Sandy-Smith, K. K. Tang, G. Wu, A. Zhang, and W. Zhen, "iNEMI Project on Process Development of BiSn-Based Low Temperature Solder Pastes – Part III: Mechanical Shock Tests on POP BGA Assemblies", Proceedings of the 2018 International Conference on Electronics Packaging, Kuwana, Japan, April 2018.

[4] H. Fu, J. Radhakrishnan, M. Ribas, R. Aspandiar, B. Arfaei, K. Byrd, J. Chen, S. Cheng, Q. Chen, R. Coyle, D. Daily, S. Feng, M. Krmpotich, S. Mokler, B. Sandy-Smith, K. K. Tang, G. Wu, A. Zhang, and W. Zhen, "iNEMI Project on Process Development of BiSn-Based Low Temperature Solder Pastes – Part IV: Comprehensive Mechanical Shock Tests on POP Components Having Mixed BGA BiSn-SAC Solder Joints", To be presented at the 2018 SMTA International Conference, Rosemont, IL, October 2018.

[5] Aspandiar, R., Byrd, K., Tang, K. K., Campbell, L., and Mokler, S., "Investigation of Low-temperature Solders to Reduce Reflow temperature, Improve SMT Yields and Realize Energy Savings." Proceedings of the IPC APEX EXPO. San Diego, California. February 2015.

[6] Chen, O. H., Byrd, K., Mokler, S., Tang, K. K., and Aspandiar, R., "Comparison of the Mechanical Shock/Drop Reliability of Flip Chip BGA (FCBGA) Solder Joints Formed by Soldering with Low-temperature BiSn-Based Resin Reinforced Solder Pastes." Proceedings of the International Conference on Soldering and Reliability. Markham, Ontario. May 2015.

[7] Chen, O. H., Molina, A., Aspandiar, R., Byrd, K., Mokler, S., and Tang, K. K., "Mechanical Shock and Drop Reliability Evaluation of the BGA Solder Joint Stack-Ups Formed by Reflow Soldering SAC Solder Balls BGAs with BiSnAg and Resin Reinforced BiSn-Based Solder Pastes." Proceedings of the SMTA International Conference and Exhibition. Rosemont, Illinois. September 2015.

[8] Mokler, S., Aspandiar, R., Byrd, K., Chen, O., Walwadkar, S., Tang, K. K., Renavikar, M., and Sane, S., "The Application of Bi-Based Solders for Low-temperature Reflow to Reduce Cost While Improving SMT Yields in Client Computing Systems." Proceedings of the SMTA International Conference and Exhibition. Rosemont, Illinois. September 2016.

[9] S. Sahasrabudhe, S. Mokler, M. Renavikar, S. Sane, K. Byrd, E. Brigham, O. Jin, P. Goonetilleke, N. Badwe and S. Parupalli, "Low Temperature Solder – A Breakthrough Technology for Surface Mounted Devices", Proceedings of the 2018 IEEE 68th Electronic

Components and Technology Conference, 2018, pp.1455-1464.
[10] Board Assembly Chapter, 2017. "iNEMI Roadmap." www.inemi.org/inemi-roadmap.
[11] National Center for Manufacturing Sciences. "Lead-Free Solder Project Final Report." Report 0401RE96, May 1997.
[12] Mei, Z., Holder, H. A., and Vander Plas, H. A. "Low-Temperature Solders." *Hewlett-Packard Journal*, Article 10, August 1996, pp. 1–10.
[13] Ribas, M., Chegudi, S., Kumar, A., Pandher, R., Raut, R., Mukherjee, S., Sarkar, S., and Singh B., "Development of Low-Temperature Drop Shock Resistant Solder Alloys for Handheld Devices." Proceedings of the IEEE 15th Electronics Packaging Technology Conference. Singapore. December 2013, pp. 53–57.
[14] Ribas, M., Kumar, A., Kosuri, D., Rangaraju, R. R., Choudhury, P., Telu, S., and Sarkar, S., "Low-temperature Soldering Using Sn-Bi Alloys." Proceedings of the SMTA International Conference and Exhibition. Rosemont, Illinois. September 2017.
[15] Ribas, M. "Advancements in Low-temperature Soldering." *SMT Today*, September 2017, pp. 36–38.
[16] Ribas, M., Hunsinger, T., Cucu, T., Ramakrishna, H. V., Lim, G. and Murphy, M., *The Printed Circuit Assembler's Guide to...Low-Temperature Soldering*, BR Publishing, Inc., 2018. Retrieved from http://i007ebooks.com/my-i- connect007/books/lts/.
[17] ASTM Standard E794, "Standard Test Method for Melting and Crystallization Temperatures by Thermal Analysis", ASTM International, 2012.
[18] ASTM Standard E8, "Standard Test Methods for Tension Testing of Metallic Materials", ASTM International, 2011.
[19] IPC Standard 7095A, "Design and Assembly Process Implementation for BGAs", IPC Association, October 2004.
[20] IPC Standard TM-650 2.4.43, "Test Methods Manual", IPC Association, January 1995.
[21] JEDEC Standard JESD22-B111A, "Board Level Drop Test Method of Components for Handheld Electronic Products", IPC Association, July 2003.
[22] IPC/JEDEC Standard 9706, "Mechanical Shock In-situ Electrical Metrology Test Guidelines for FCBGA SMT Component Solder Crack and Pad Crater/Trace Crack Detection", JEDEC Solid State Technology Association, December 2013.
[23] Ribas, M., Chegudi, S., Kumar, A., Pandher, R., Mukherjee, S., Sarkar, S., Raut, R., and Singh B., "Comprehensive Report on Low-temperature Solder Alloys for Portable Electronics." Proceedings of the SMTA International Conference and Exhibition. Rosemount, Illinois. September 2015, pp. 176–183.